OPTICAL, PHOTOCATALYTIC AND THERMOELECTRIC PROPERTIES OF Cu_2MeSnS_4 (Me=Mn^{2+}, Fe^{2+}, Co^{2+}) NANOCRYSTALS VIA MICROWAVE-ASSISTED SOLVOTHERMAL METHOD

H. GUAN*, X. WANG, Y. HUANG
School of Materials Science and Engineering, Yancheng Institute of Technology, 9 Yinbing Street, Yancheng 224051, PR China

Quaternary semiconductor Cu_2MeSnS_4(Me=Mn^{2+}, Fe^{2+}, Co^{2+}) nanocrystals were synthesized via microwave-assisted solvothermal method for the first time. These nanocrystals were characterized by X-ray diffraction (XRD), Raman spectroscopy, scanning electron microscopy (SEM) and UV-vis-NIR spectroscopy. The band gaps of 1.1-1.2eV and better photocatalytic properties (the degradation of methylene blue(MB) could reach up to about 53, 85 and 61%, repectively) indicate that Cu_2MeSnS_4(Me=Mn^{2+}, Fe^{2+}, Co^{2+}) nanocrystals are ideal for applications in low-cost thin-film solar cells and solar photocatalysts. In addition, bulk Cu_2MeSnS_4(Me=Mn^{2+}, Fe^{2+}, Co^{2+}) samples can be used in high-temperature thermoelectric devices owing to their high electrical conductivities and large Seebeck coefficients.

(Received June 4, 2018; Accepted September 1, 2018)

Keywords: Microwave-assisted solvothermal method, Cu_2MnSnS_4, Cu_2FeSnS_4, Cu_2CoSnS_4, Solar cells, Photocatalyst, Thermoelectric device

1. Introduction

In recent decades, with the development of indutrialization, the energy crisis and water pollution have become urgent problems. Searching for environmentally-friendly advanced technologies has attracted interest of many researchers. As a novel chalcogenide semiconductor for energy conversion, Cu_2ZnSnS_4 (CZTS) containing abundant and non-toxic elements exhibits outstanding photovoltaic, photocatalytic and thermoelectric properties due to its suitable band gap(~1.5eV) , high absorption coefficient (>10^4cm^{-1}) and low lattice thermal conductivity [1-8]. We believe that transition metal-based Cu_2MeSnS_4(Me=Mn^{2+}, Fe^{2+}, Co^{2+}) quaternary chalcogenide semiconductors are also considered as energy conversion materials owing to their low band-gap energies, optical absorption coefficients(> 10^4cm^{-1}) and low lattice thermal conductivities similar to that of CZTS.

Several methods have been used for the synthesis of chalcogenide materials, such as hot-injection method, solvothermal method, colloidal method, microwave-assisted solvothermal method and so on [9-15]. As a novel solution-based method, microwave-assisted solvothermal method gains popularity owing to its fast heating rate, low pressure, short reaction duration and superior repeatability. As far as we know, no reports have been found to synthesize Cu_2MeSnS_4(Me=Mn^{2+}, Fe^{2+}, Co^{2+}) nanocrystals via microwave-assisted solvothermal method.

In this paper, we synthesized Cu_2MeSnS_4(Me=Mn^{2+}, Fe^{2+}, Co^{2+}) nanocrystals via microwave-assisted solvothermal method, and investigated their structure, morphology, optical, photocatalytic and thermoelectric properties.

2. Experimental details

$CuCl_2·2H_2O$(AR), $Mn(CH_3COO)_2·4H_2O$(AR), $Fe(NO_3)_3·9H_2O$(AR), $Co(CH_3COO)_2·6H_2O$(AR), $SnCl_2·2H_2O$ (AR) and H_2NCSNH_2(AR) were used as raw materials. In a typical experiment, $CuCl_2·2H_2O$ (0.025M), $Mn(CH_3COO)_2·4H_2O$ ($Fe(NO_3)_3·9H_2O$,

*Corresponding author: guanhao1980@sina.com

$Co(CH_3COO)_2 \cdot 6H_2O$) (0.0125M) , $SnCl_2 \cdot 2H_2O$ (0.0125M) and H_2NCSNH_2 (0.05M) were added in 40ml ethylenediamine to dissolve under magnetic stirring. The solution was then transfered into Teflon Vessels and putted into a microwave oven(2.45GHz, 800W) heat to 230℃ in 30min and maintained for 2h. After the reaction, the as-obtained products were washed several times with deionized water and dried in vacuum at 80℃ for 3h.

In a photocatalystic experiment, 0.05g of Cu_2MeSnS_4(Me=Mn^{2+}, Fe^{2+}, Co^{2+}) was added to 50ml of MB solution with the concerntration of 10^{-5}mol/l. Then the solution was stirred in the dark for 30min ensure the balance of adsorption and desorption of MB before the ones exposed to visible light irradiation under sustained stirring. At given time intervals, 5ml of the as-obtained solution were used as measured samples after removing Cu_2MeSnS_4(Me=Mn^{2+}, Fe^{2+}, Co^{2+}) nanocrystals by centrifugation. In a thermoelectric experiment, Cu_2MeSnS_4(Me=Mn^{2+}, Fe^{2+}, Co^{2+}) nanocrystals were utilized to prepare pellet samples by hot-pressing sintering.

The crystal structure was characterized using a PANalytical X'Pert PRO diffractometer with Cu$K\alpha$ radiation (λ=0.15406nm) and JY-T64000 Raman spectrometers. The microstructure was investigated using LEO-1530VP scanning electron microscope. The optical property was measured using Varian Cary 5000 spectrophotometer. The photocatalytic property was measured using Shimadzu UV2450 spectrophotometer. The thermoelectric properties were measured using Namicro-β thermoelectric parameters measurement.

3. Results and discussion

The XRD patterns of Cu_2MeSnS_4(Me=Mn^{2+}, Fe^{2+}, Co^{2+}) are shown in Fig.1(a). It can be seen that all diffraction peaks of as-obtained Cu_2MeSnS_4 nanocrystals at 2θ=~28°, ~47° and ~56° corresponding to (112), (204) and (312) planes of stannite Cu_2MeSnS_4(Me=Mn^{2+}, Fe^{2+}, Co^{2+}), indicating that pure Cu_2MeSnS_4(Me=Mn^{2+}, Fe^{2+}, Co^{2+}) phases are obtained. The broad diffraction peaks of the samples show the small size of the Cu_2MnSnS_4(CMTS), Cu_2FeSnS_4(CFTS) and Cu_2CoSnS_4(CCTS) nancrystals. According to the Debye-Scherrer formula, the average crystallite size of CMTS, CFTS and CCTS nanocrystals can be calculated to be about 13.05nm, 6.75nm and 8.69nm, respectively.

The phase purity of the Cu_2MeSnS_4(Me=Mn^{2+}, Fe^{2+}, Co^{2+}) nanocrystals was further studied by Raman analysis. It can be seen from Fig.1(b) that the Raman spectra exhibit some major peaks (between 327cm^{-1} and 329cm^{-1}) with broadness, which are nearly related to the values obtained in the literature [16-18]. In addition, the peaks belonging to the possible impurity phase such as Cu_2SnS_3 (290, 318 and 348 cm^{-1}) are not detected, demonstrating that all of the samples had high purity [19].

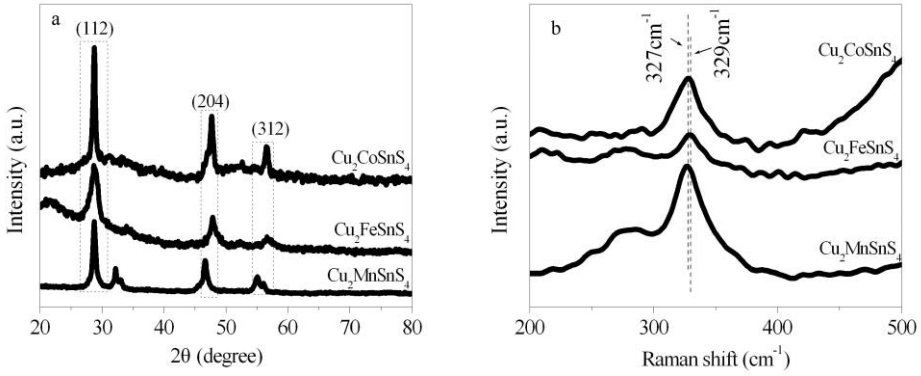

Fig. 1 XRD patterns (a) and Raman spectra (b) of Cu_2MeSnS_4(Me=Mn^{2+}, Fe^{2+}, Co^{2+}) nanocrystals

The morphologies of Cu_2MeSnS_4(Me=Mn^{2+}, Fe^{2+}, Co^{2+}) are shown in Fig.2. Under SEM observations, CMTS and CCTS exhibit irregular particles being composed of large numbers of nanocrystals with an average size of about 10~15nm but they are agglomerated. The result is caused by the high surface energy of nanocrystals due to their small sizes[4]. In contrast, CFTS

display sheet-like structure being composed of small nanocrystals with the average size of about 8nm. For CMTS and CCTS, the precursors react and nucleate rapidly, afterward small nanocrystals form bigger aggregates. For CFTS, the relatively lower reaction rate provides an ideal condition for the anisotropic growth. CFTS nanocrystals maybe partially disperse and dissolve, and further grow up to sheet-like structure through oriented aggregation [20-21].

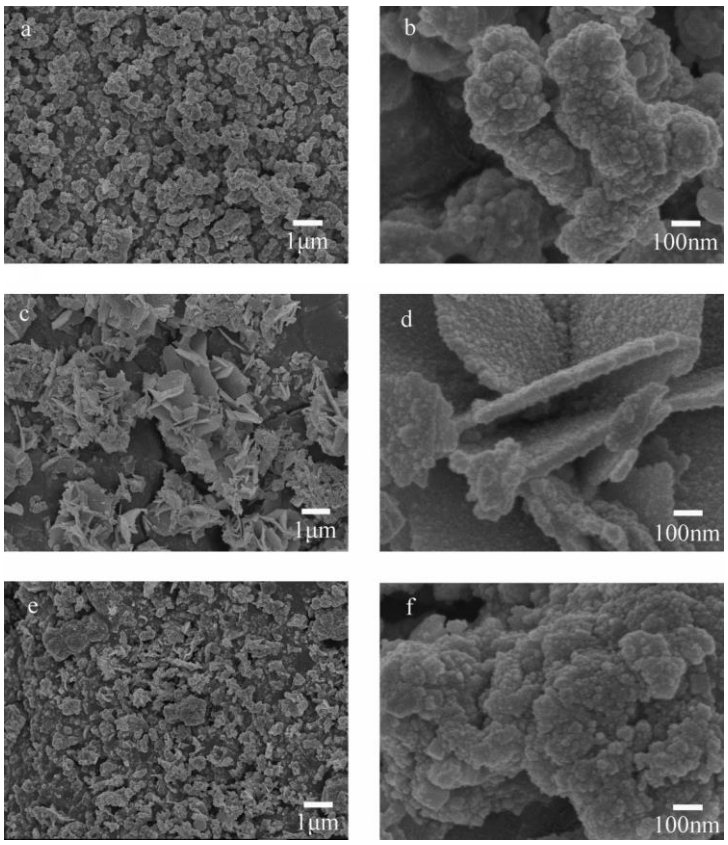

Fig. 2. Low magnification and high magnification SEM images of Cu_2MeSnS_4(Me=Mn^{2+}, Fe^{2+}, Co^{2+}) nanocrystals(a, b) Cu_2MnSnS_4; (c, d) Cu_2FeSnS_4; (e, f) Cu_2CoSnS_4

In order to investigate the optical properties, UV-vis-NIR spectroscopy was carried out for Cu_2MeSnS_4(Me=Mn^{2+}, Fe^{2+}, Co^{2+}) nanocrystals. The strong and broad optical absorption in the visible range can be observed from Fig.3. As shown in the set, the optical band gaps of the Cu_2MeSnS_4(Me=Mn^{2+}, Fe^{2+}, Co^{2+}) nanocrystals can be estimated from the $(\alpha h\nu)^2$ versus $h\nu$. The values are around 1.11eV, 1.14eV and 1.22eV, respectively. Note that the optical band gaps are in the range of 1.1-1.2eV. Compared with bulk CZTS materials(~1.5eV), the measured band gaps are shift due to quantum confinement effect and composition variation of the nanostructure the samples [12, 22-23]. The values further eliminate the existence of Cu_2S and Cu_2SnS_3. The as-obtained values indicate the suitable optical properties for photovoltaic applications.

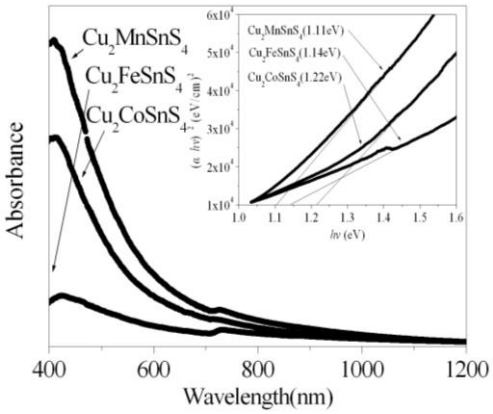

Fig. 3 UV-vis-NIR absorption spectra of Cu_2MeSnS_4(Me=Mn^{2+}, Fe^{2+}, Co^{2+}) nanocrystals
Inset: Optical band gap estimations of Cu_2MeSnS_4(Me=Mn^{2+}, Fe^{2+}, Co^{2+}) nanocrystals

The decomposition of methylene blue(MB) under visible-light irradiation for different time were examined to evaluate the photocatalytic properties of Cu_2MeSnS_4(Me=Mn^{2+}, Fe^{2+}, Co^{2+}) nanocrystals. The photocatalytic degradation rates(C/C_0) of the MB with and without Cu_2MeSnS_4(Me=Mn^{2+}, Fe^{2+}, Co^{2+}) nanocrystals are shown in Fig.4, where C be the concentration of MB under visible-light irradiation for a certain time and C_0 be the concentration of MB after the adsorption-desorption equilibrium on the catalysts before irradiation. After 100min of visible-light irradiation, MB without catalyst decomposes only about 3%, indicating that self-degradation of MB could be neglected. While about 53, 85 and 61% of MB were decomposed by Cu_2MeSnS_4(Me=Mn^{2+}, Fe^{2+}, Co^{2+}) nanocrystals, respectively. The higher photodegradation efficiencies may be attributed to their narrow band gaps and strong small size effects. The photocatalytic degradation rate of CFTS nanocrystals is better than that of CMTS and CCTS nanocrystals due to large surface areas, which is in accordance with SEM images. This property exhibits a potential candidate for visible-light photocatalysts.

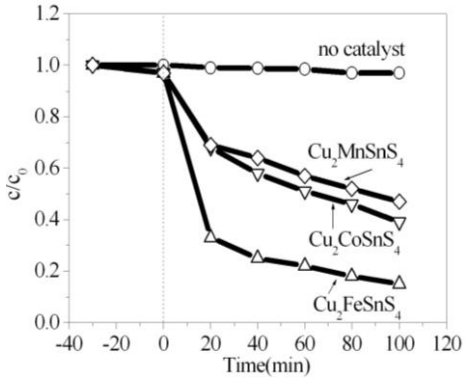

Fig. 4. The photodegradation rates of MB as a function of different time with and without the addition of Cu_2MeSnS_4(Me=Mn^{2+}, Fe^{2+}, Co^{2+}) nanocrystals

The curves of temperature dependent electrical conductivities(σ) and Seebeck coefficients(S) of Cu_2MeSnS_4(Me=Mn^{2+}, Fe^{2+}, Co^{2+}) nanocrystals are shown in Fig.5. It can be seen that these nanocrystals show *P*-type nature due to the positive values of Seebeck coefficient. With the temperature increasing, the electrical conductivities and Seebeck coefficients also increase. The electrical conductivities of Cu_2MeSnS_4(Me=Mn^{2+}, Fe^{2+}, Co^{2+}) nanocrystals could reach up to 16.24S•m^{-1}, 15.37S•m^{-1} and 19.85S•m^{-1} at 675*K*, respectively, which are closely

related to their narrow band-gaps. The Seebeck coefficients of Cu_2MeSnS_4(Me=Mn^{2+}, Fe^{2+}, Co^{2+}) nanocrystals could reach up to 139.73μV•K^{-1}, 123.65μV•K^{-1} and 176.93μV•K^{-1} at 675*K*, respectively, which are attributed to spin entropy of magnetic ions Mn^{2+}, Fe^{2+} and Co^{2+}.

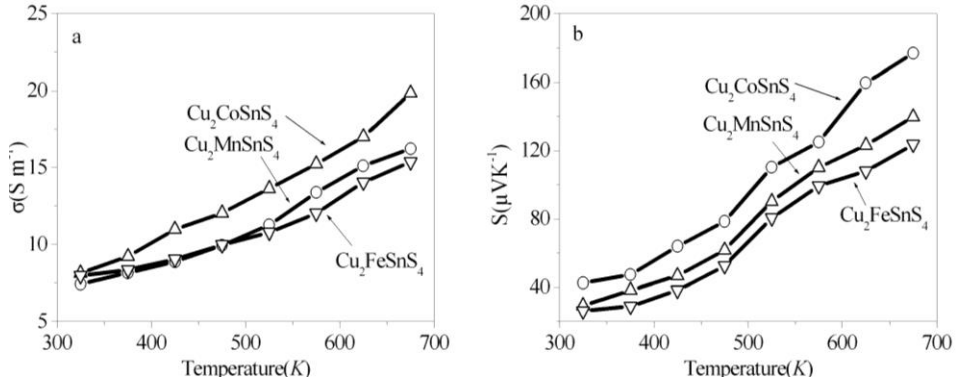

Fig. 5 Temperature-dependent plot of (a) electrical conductivities and (b) Seebeck coefficients of Cu_2MeSnS_4(Me=Mn^{2+}, Fe^{2+}, Co^{2+}) nanocrystals samples

4. Conclusions

In summary, three types of quaternary Cu_2MeSnS_4(Me=Mn^{2+}, Fe^{2+}, Co^{2+}) semiconductor nanocrytals have been firstly synthesized via microwave-assisted solvothermal apporach. These semiconductor nanocrystals have optical band gaps of 1.1-1.2eV and degrade about 53, 85 and 61% of MB within 100min under visible-light irradiation, respectively, indicating that these nanocrystals have potential applications in the fields of photovatic and photocatalysis. The high electrical conductivities and large Seebeck coefficients of as-obtained bulk Cu_2MeSnS_4(Me=Mn^{2+}, Fe^{2+}, Co^{2+}) samples show that these samples can be useful for applications in high-temperature thermoelectric devices.

Acknowledgements

This research is financial supported by Top-notch Academic Programs Project of Jiangsu Higher Education Institutions (PPZY2015A025).

References

[1] B. Shin, O. Gunawan, Y. Zhu, N. A. Bojarczuk, S. Jay Chey, S. Guha, Prog. Photovolt: Res. Appl. **1**, 72 (2013)
[2] J. Huang, C. Yan, K. Sun, F. Liu, H. Sun, A. Pu, X. Liu, M. Green, X. Hao, Sol. Energy Mater. Sol. Cells **175**, 71 (2018)
[3] K. Wang, O. Gunawan, T. Todorov, B. Shin, S. J. Chey, N. A. Bojarczuk, D. Mitzi, S. Guha, Appl. Phys. Lett. **97**, 143508 (2010)
[4] Y. Gao , F. Long, J. Wang, J. Zhang, S. Mo, Z. Zou, Mater. Design **123**, 24 (2017)
[5] R. Chong, X. Wang, Z. Chang, W. Zhou, S. Wu, Int. J. Hydrogen Energy **42**, 20703 (2017)
[6] M. Z. Ansari, M. Faraz, S. Munjal, V. Kumar, N. Khare, Adv. Powder Tech. **28**, 2402 (2017)
[7] M. Zubair, A. Razzaq, C. A. Grimes, S. In, J CO_2 Util. **20**, 301 (2017)
[8] H. R. Yang, L. A. Jauregui, G. Q. Zhang, Y. P. Chen, Y. Wu, Nano. Lett.. **12**, 540 (2012)
[9] Y. Cui, R. Deng, G. Wang, D. Pan, J. Mater. Chem. **22**, 23136 (2012)
[10] A. Kamble, K. Mokurala, A. Gupta, S. Mallick, P. Bhargava, Mater. Lett. **137**, 440 (2014)
[11] X.Y. Zhang, N. Z. Bao, B. P. Lin, G. Arunava, Nanotechnology **24**, 105706 (2013)

[12] F. Ozel, E. Aslan, B. Istanbullu, O. Akay, I. H. Patir, Appl. Catal. B: Environ. **198**, 67 (2016)
[13] Z. Zou, Y. Gao, F. Long, J. Wang, J. Zhang, Mater. Lett **158**, 13 (2015)
[14] Y. Lin, S. Das, C. Yang, J. Sung, C. Lu, J. Alloy. Compd. **632**, 354 (2015)
[15] B. Patro, S. Vijaylakshmi, P. Sharma, J. Mater. Sci.: Mater. Electron.**4**, 3370 (2018)
[16] L. L. Chen, H .M. Deng, J. H. Tao, W. L. Zhou, L. Sun, F. Y. Yue, P. X. Yang, J. H. Chu, J. Alloys Compd. **640**, 23 (2015)
[17] H. Guan, H. Shen, B. Jiao, X. Wang, Mater. Sci. Semicon. Proc. **25**, 159 (2014)
[18] J. Zhong, Q. Wang, W. Cai, Mater. Lett **150**, 69 (2015)
[19] Q. Luo, Y. Q. Zeng, L. W. Chen, C. Q. Ma, Chem. Asian. J. **9**, 2309 (2014)
[20] Y. L. Zhou, W. H. Zhou, M. Li, Y. F. Du, S. X. Wu, J. Phys. Chem. C **115**, 19632 (2011)
[21] S. Bahramzadeh, H. Abdizadeh, M. R. Golobostanfard, J. Alloy. Compd. **642**, 124 (2015)
[22] Z. Su, C. Yan, D. Tang, K. Sun, Z. Han, F. Liu, Y. Lai, J. Li, Y. Liu, Cryst. Eng. Commun. **14**, 782 (2012)
[23] A. Gillorin, A. Balocchi, X. Marie, P. Dufoura, J. Y. Chane-Ching, J. Mater. Chem. **21**, 5615 (2011)